Direct Observation by Neutron Diffraction of Antiferromagnetic Ordering in *s* Electrons Confined in Regular Nanospace of Sodalite

Takehito Nakano,[1,*] Masato Matsuura,[2,†] Atsufumi Hanazawa,[1] Kazuma Hirota,[2] and Yasuo Nozue[1]

[1]*Department of Physics, Graduate School of Science, Osaka University, Osaka 560-0043, Japan*

[2]*Department of Earth and Space Science, Graduate School of Science, Osaka University, Osaka 560-0043, Japan*

(Received 29 August 2011; published 17 October 2012)

Sodium clusters formed in the regular nanospace of sodalite (aluminosilicate zeolite) are known to show antiferromagnetic order without any magnetic elements. The clusters are arrayed in a body centered cubic structure. We have performed a neutron diffraction study and succeeded in detecting the magnetic Bragg peaks of the *s*-electron spins for the first time. The observation of both 001 and 111 magnetic reflections confirms the antiferromagnetic order with the antiparallel coupling between the nearest neighbor clusters. The magnetic form factor was examined by analyzing the intensity ratios of the magnetic and nuclear Bragg peaks. The result is in good agreement with the shape of the *s*-electron wave function derived from theoretical studies of the sodium nanoclusters in the cages.

DOI: 10.1103/PhysRevLett.109.167208 PACS numbers: 75.50.Ee, 71.20.Dg, 75.25.−j, 82.75.Vx

Magnetic ordering is typically exhibited by *d*- and *f*-electron systems, because the localized features of their wave functions tend to stabilize the localized magnetic moments and/or narrow the energy bands. In the past decades, great effort has been made to find magnetic ordering in materials comprising only nonmagnetic elements. One representative example is purely organic magnets as *p*- (or π-) electron systems [1–4]. Another is three-dimensionally arrayed alkali-metal nanoclusters in zeolites as *s*-electron systems [5–10]. Zeolites are porous aluminosilicate crystals possessing regularly arrayed nanospaces with rich varieties of structure. The alkali-metal clusters are generated by loading guest alkali atoms, where the *s* electrons are shared by several alkali cations and confined in ''cages'' formed by the zeolite framework. In some cases, clusters can be magnetic and the mutual interaction among the arrayed clusters realizes various kinds of magnetic orderings, such as ferromagnetism, antiferromagnetism, and ferrimagnetism, depending on the crystal structure of the host cage and the species of the guest alkali element [5–10]. These results demonstrate that *s*-electron systems can be magnetic materials when the localized character and mutual interactions are set appropriately by confining the *s* electrons in regular nanospace, although *s* electrons usually form delocalized energy bands in bulk alkali metals and show only Pauli paramagnetism. Thus, these systems are a new class of magnetic material. The magnetic ordering has been confirmed by several tools including microscopic magnetic probes [11–17]. However, there have been no reports on determining the magnetic structures of alkali-metal clusters arrayed in zeolites. This may be due to the large unit cell and a resultant low spin density. In the present work, we carried out a neutron diffraction (ND) study on the antiferromagnetic (AFM) state of sodium clusters arrayed in sodalite crystal possessing the simplest structure among the zeolite family. We report the first direct observation of long-range magnetic ordering of *s* electrons by ND. The magnetic structure and the shape of the *s*-electron wave function in the sodium cluster are also examined.

As shown in Fig. 1(a), the sodalite framework is built of oxygen-sharing AlO_4 and SiO_4 tetrahedrons, where β cages with an inside diameter of about 7 Å are arrayed in a body-centered cubic (bcc) structure with a lattice constant of 8.9 Å. Two β cages are contained in the bcc unit cell. Adjacent β cages are connected through six-membered rings. The chemical formula of salt-free sodalite, namely, hydrosodalite, is given by $Na_6(AlSiO_4)_6xH_2O$ per unit cell. Three Na^+ ions are accommodated in each β cage. By exposing the dehydrated sodalite to sodium vapor, one Na atom is adsorbed in the β cage and an Na_4^{3+} cluster is formed [18]. In this cluster, one *s* electron provided by the guest Na atom is equivalently shared by four Na^+ ions and confined in the β cage as shown in Fig. 1(b). Srdanov and co-workers succeeded in forming Na_4^{3+} clusters in almost all the β cages, that is, nearly 100% doping with a chemical formula of $Na_8(AlSiO_4)_6$, and found AFM order below the Néel temperature of $T_N = 48$ K [7]. The

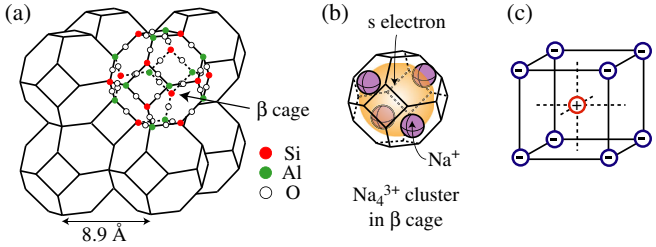

FIG. 1 (color online). Schematic illustrations of (a) crystal structure of sodalite, (b) Na_4^{3+} cluster formed in the β cage, and (c) magnetic structure model of Na clusters in sodalite. The electronic spin in the body center cluster and that in the corner cluster are coupled in antiparallel in the bcc lattice.

magnetic phase transition has also been confirmed by ^{27}Al- and ^{29}Si-NMR [11,12], and by μSR [14]. Several theoretical studies predicted a magnetic structure where the spin in the body center cluster and that in the corner cluster are antiferromagnetically coupled as shown in Fig. 1(c) [19–22]. However, direct experimental evidence of the magnetic structure has not yet been obtained, although the same structure has been implicitly assumed in the analysis of magnetic susceptibility [11,16].

We used a powder specimen of sodalite synthesized by Tosoh Corporation. Each crystal size is a few micrometers. The salt-free sodalite powder was heated to 500 °C in a vacuum for 24 h and fully dehydrated. Dehydrated powder was sealed in a quartz glass tube with distilled Na metal. Na was adsorbed into the zeolite at 160 °C for 2 weeks. The magnetic susceptibility (χ) was measured by a superconducting quantum interference device magnetometer (MPMS-XL, Quantum Design). We confirmed that the temperature dependence of χ was in good agreement with that in several reported works [7,12,14–16]. For ND experiments, a powder of 2.2 grams was put in a vanadium-film cylinder, 15-mm diameter, and sealed in an aluminum can filled with He gas. This process was performed under a pure He atmosphere in a glove box and the sample was never exposed to the air. ND experiments were performed using the spectrometer PONTA at the JRR-3 reactor at the Japan Atomic Energy Agency. Pyrolytic graphite (PG) crystals were used as the monochromator and the analyzer. The energy of the incident beam was set at 14.7 meV (wavelength $\lambda = 2.36$ Å). A PG filter was placed before the sample to remove higher-order contaminations. The horizontal collimation of the incident and scattered neutron beam was 80 min.

Figure 2(a) shows a powder ND pattern of Na-loaded sodalite taken at 4 K. As shown later, the magnetic reflections are extremely weak, and the ND pattern shown in Fig. 2(a) is well explained by nuclear reflections. The red solid curve in Fig. 2(a) shows a Rietveld analysis result based on the structural parameters reported by Madsen and co-workers with the space group $P\bar{4}3n$ [20]. A lattice constant of $a = 8.921(7)$ Å, and reliability factors of $R_{\mathrm{wp}} = 4.98\%$, $R_p = 3.53\%$ and $S = 1.12$ are obtained. A small peak observed at $2\theta = 46.4°$ is due to the 110 reflection of Na metal. This is only 1 wt% of the total weight of the sample, indicating that a very small amount of Na metal is adhered to the surface of the crystals. In order to check the existence of magnetic reflections, we recorded much higher statistics data at the scattering angle regions around the 001 and 111 reflections at various temperatures. These are forbidden in the nuclear reflections based on the crystal structure. Figure 2(b) shows ND data around the 001 reflection taken at 4 and 56 K, corresponding to below and above T_N, respectively. Figure 2(c) represents the difference plot between them, namely, $I_{4\,\mathrm{K}}$–$I_{56\,\mathrm{K}}$. The 001 reflection is clearly observed at low

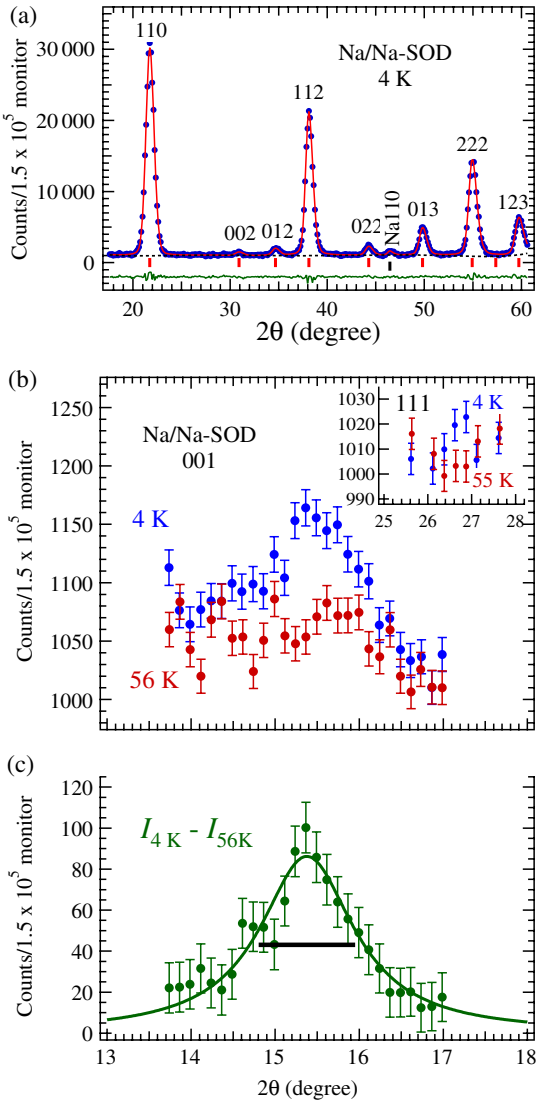

FIG. 2 (color online). (a) Powder ND pattern of Na-loaded sodalite taken at 4 K. The counting time for each datum point was 30 sec. The red solid curve shows a Rietveld analysis result with considering only nuclear reflections by utilizing RIETAN-2000 [26]. The magnetic reflections are too weak to be observed in the data. (b) ND data at the scattering angle region around the 001 reflection at temperatures below and above T_N. The counting time for each datum point was 5 min. The inset shows the data for the 111 reflection. The counting time for each datum point was 30 min. (c) Difference plot for the 001 reflection between the data taken at 4 and 56 K. The horizontal bar indicates the angular resolution in the present experimental setup.

temperature, where the intensity is nearly three orders of magnitude weaker than that of the 110 nuclear reflection. This is not due to higher-order (e.g., $\lambda/2$) contaminations of the incident neutron beam because the relative intensity of the 001 peak was not reduced when we added a PG filter after the sample. We evaluated the total count of scattered neutrons at $13.7° \leq 2\theta \leq 17.0°$, and this is plotted as a function of temperature in Fig. 3. The count is almost

constant at high temperature, but suddenly increases below about 50 K, which coincides well with T_N. The solid curve in Fig. 3 shows the calculation result using a phenomenological equation of the order parameter, $I(T) = I(0)[1 - (T/T_N)]^{2\beta}$ with a constant background. The Néel temperature $T_N = 48 \pm 3$ K and the exponent $\beta = 0.37 \pm 0.06$ were obtained. The value of β is typical for a three-dimensional (3D) Heisenberg system. Similar values were also reported in μSR studies [14]. These results indicate that the observed 001 peak at low temperature is a magnetic reflection originating from the AFM order of s electrons confined in the sodalite cages.

As seen in Fig. 2(c), the 001 reflection peak has a rather long tail. The difference plot is well reproduced by a Lorentzian function, as shown by the solid curve. The horizontal bar in Fig. 2(c) indicates the angular resolution of our experimental setup. The peak width of the difference plot is almost the same as the resolution. Therefore, antiferromagnetism in Na-loaded sodalite can be regarded as a long-range ordering. As shown in the inset of Fig. 2(b), the 111 reflection is also weakly observed at $2\theta \approx 26.5°$ below T_N. This is also regarded as a magnetic reflection because it is forbidden as a nuclear reflection based on the crystal structure. The simultaneous observation of 001 and 111 magnetic Bragg peaks strongly supports the simple magnetic structure shown in Fig. 1(c) with the propagation vector of (0,0,1) [23]. AFM resonance studies suggest a very weak magnetic anisotropy [16,17]. However, we cannot determine the magnetic easy axis in our powder ND experiment because the crystal has a cubic symmetry.

From the ratio of the integrated intensity of the 001 magnetic Bragg peak to the 110 nuclear one, the ordered magnetic moment was evaluated to be $0.72 \pm 0.02\mu_B$ (Bohr magneton) at 4 K. However, the value of $0.42 \pm 0.15\mu_B$ was evaluated by the same method from the 111 magnetic Bragg peak. This inconsistency must be origineted from the scattering vector q dependence of magnetic form factor f_m, because the magnetic Bragg peak intensity is proportional to $|\mu \cdot f_m|^2$, where μ is the ordered magnetic moment. Examining f_m is crucial to understand the magnetism of this s-electron system because of the following reasons. In contrast to the atomic orbitals of d and f electrons in ordinary magnets, the shape of the s-electron wave function responsible for the magnetic moment in this system is non-trivial, because the wave function may be delocalized over a nanometer size in the cluster. According to the theoretical predictions [22,24], the spatial distribution of the s-electron wave function plays a key role in the exchange coupling in this system. This is because the spatial distribution directly affects the on-site (on-cluster) Coulomb repulsion energy and also the overlapping between the wave functions of adjacent clusters.

According to the $\chi - T$ data above T_N, each β cage accommodates one unpaired electronic spin with $s = 1/2$ and $g = 2$ [12,14–16]. Moreover, μSR and AFM resonance studies confirmed that this system is an ideal 3D Heisenberg type [14,16]. Therefore, it is appropriate to assume $\mu = 1\mu_B$ because a spin fluctuation is expected to be less in 3D systems. In Fig. 4, the obtained f_m for the 001 and 111 reflections are plotted as a function of $q(= 4\pi \sin\theta/\lambda)$ by closed circles. The simplest model describing the electron wave function of the cluster is the "particle-in-a-spherical-box" model where an electron is confined in a spherical-well potential [25]. In the sodalite system, one unpaired electron occupies the $1s$ ground state of the cluster in a β cage. In this model, the $1s$ wave function is given by $\Psi_{1s}(r) = (1/\sqrt{2\pi a})[\sin(\pi r/a)/r]$.

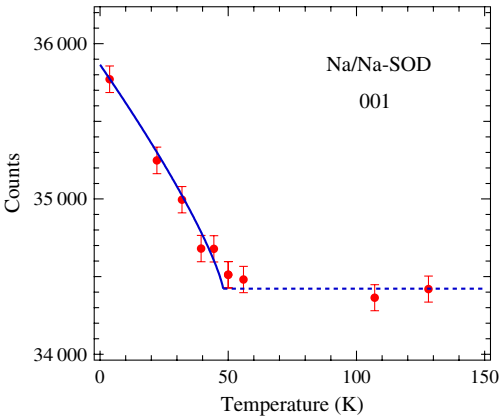

FIG. 3 (color online). Temperature dependence of the integrated intensity of the 001 Bragg peak. The solid curve represents a calculation using a phenomenological equation of the order parameter.

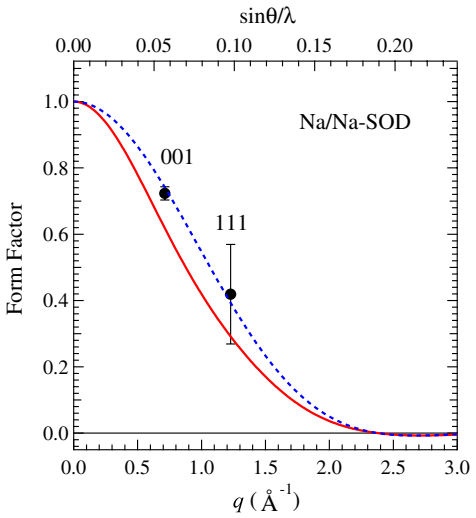

FIG. 4 (color online). Magnetic form factor f_m of Na clusters in sodalite for scattering vector q. The closed circles show experimental results obtained by 001 and 111 reflections. The dotted curve represents the form factor of the $1s$ wave function calculated by assuming a spherical-well potential with an inside diameter of 7 Å. The solid curve is calculated by using the maximally localized Wannier orbital reported by Nakamura *et al.* [24].

By assuming the inside diameter of the β cage as $2a = 7$ Å, we calculate the form factor, which is plotted by the dashed curve in Fig. 4. Recently, Nakamura and co-workers performed *ab initio* calculations based on the density functional theory and derived a maximally localized Wannier orbital which corresponds to the *s*-like electron wave function confined in a β cage [24]. By utilizing the numerical data of this Wannier orbital, we calculated the form factor, and this is plotted in Fig. 4 by the solid curve. The calculation results are in rather good agreement with the experimental ones. It is difficult to choose the one of these two theoretical models only from the present experimental data. However, the commonality of these two models is that the electron wave function is confined in the nanosized cage. Therefore, it is evident that the *s* electron responsible for the magnetic moment under AFM order possesses a wave function delocalized over a nanometer size in the cluster and confined in the cage as schematically represented in Fig. 1(b). This is the first direct information on the spatial distribution of electron spin in zeolite systems. However, to more reliably confirm the shape of the wave function, higher statistics data for the 111 and higher order reflections is required, because these data are very important for the estimation of detailed shape of spatial distribution of electron spin. Their intensities, however, are extremely weak. This is a challenging future study which should allow a deeper understanding of the magnetism of *s*-electron systems.

In conclusion, we performed ND experiments on the AFM state of Na clusters incorporated in sodalite and succeeded in detecting the magnetic Bragg peaks for the first time. The observed 001 and 111 magnetic peaks confirm the AFM structure with antiparallel coupling of the body center and the corner clusters in the bcc lattice. The magnetic form factor coincides well with the *s*-electron wave function confined in the Na nanocluster.

We acknowledge K. Itabashi, M. Nakano, H. Ogawa (Tosoh Corporation), T. Kagayama, S. Tamiya (Osaka Univ.), K. Nakamura, and R. Arita (Univ. of Tokyo). This work was supported by Grants-in-Aid for Scientific Research on Priority Areas (No. 19051009), for Scientific Research (A) (No. 242440590) and for Young Scientists (B) (No. 20710077), and also by the Global COE Program (G10), from MEXT, Japan. The ND experiments were performed under the joint-research program of ISSP, the Univ. of Tokyo. We also thank Renovation Center of Instruments for Science Education and Technology in Osaka Univ.

*nakano@phys.sci.osaka-u.ac.jp

†Present address: Institute for Materials Research, Tohoku University, Katahira, Sendai 980-8577, Japan.

[1] S. J. Blundell and F. L. Pratt, J. Phys. Condens. Matter **16**, R771 (2004).

[2] M. Takahashi, P. Turek, Y. Nakazawa, M. Tamura, K. Nozawa, D. Shiomi, M. Ishikawa, and M. Kinoshita, Phys. Rev. Lett. **67**, 746 (1991).

[3] P.-M. Allemand, K. C. Khemani, A. Koch, F. Wudl, K. Holczer, S. Donovan, G. Gruner, and J. D. Thompson, Science **253**, 301 (1991).

[4] T. Takenobu, T. Muro, Y. Iwasa, and T. Mitani, Phys. Rev. Lett. **85**, 381 (2000).

[5] Y. Nozue, T. Kodaira, and T. Goto, Phys. Rev. Lett. **68**, 3789 (1992).

[6] T. Nakano and Y. Nozue, J. Comput. Methods Sci. Eng. **7**, 443 (2007).

[7] V. I. Srdanov, G. D. Stucky, E. Lippmaa, and G. Engelhardt, Phys. Rev. Lett. **80**, 2449 (1998).

[8] T. Nakano, K. Goto, I. Watanabe, F. L. Pratt, Y. Ikemoto, and Y. Nozue, Physica (Amsterdam) **374–375B**, 21 (2006).

[9] D. T. Hanh, T. Nakano, and Y. Nozue, J. Phys. Chem. Solids **71**, 677 (2010).

[10] T. C. Duan, T. Nakano, and Y. Nozue, J. Magn. Magn. Mater. **310**, 1013 (2007).

[11] I. Heinmaa, S. Vija, and E. Lippmaa, Chem. Phys. Lett. **327**, 131 (2000).

[12] H. Tou, Y. Maniwa, K. Mizoguchi, L. Damjanovic, and V. I. Srdanov, J. Magn. Magn. Mater. **226–230**, 1098 (2001).

[13] H. Kira, H. Tou, Y. Maniwa, and Y. Murakami, J. Magn. Magn. Mater. **226–230**, 1095 (2001).

[14] R. Scheuermann, E. Roduner, G. Engelhardt, H.-H. Klauss, and D. Herlach, Phys. Rev. B **66**, 144429 (2002).

[15] T. Nakano, R. Suehiro, A. Hanazawa, K. Watanabe, I. Watanabe, A. Amato, F. L. Pratt, and Y. Nozue, J. Phys. Soc. Jpn. **79**, 073707 (2010).

[16] T. Nakano, T. Kashiwagi, A. Hanazawa, K. Watanabe, M. Hagiwara, and Y. Nozue, J. Phys. Soc. Jpn. **78**, 084723 (2009).

[17] T. Kashiwagi, T. Nakano, A. Hanazawa, Y. Nozue, and M. Hagiwara, J. Phys. Chem. Solids **71**, 544 (2010).

[18] R. M. Barrer and J. F. Cole, J. Phys. Chem. Solids **29**, 1755 (1968).

[19] O. F. Sankey, A. A. Demkov, and T. Lenosky, Phys. Rev. B **57**, 15 129 (1998).

[20] G. K. H. Madsen, C. Gatti, B. B. Iversen, L. Damjanovic, G. D. Stucky, and V. I. Srdanov, Phys. Rev. B **59**, 12 359 (1999).

[21] R. Windiks and J. Sauer, J. Chem. Phys. **113**, 5466 (2000).

[22] G. K. H. Madsen, B. B. Iversen, P. Blaha, and K. Schwarz, Phys. Rev. B **64**, 195102 (2001).

[23] The sodalite is a cubic crystal. In the magnetic structure model shown in Fig. 1(c), three equivalent propagation vectors (1,0,0), (0,1,0), and (0,0,1) exist.

[24] K. Nakamura, T. Koretsune, and R. Arita, Phys. Rev. B **80**, 174420 (2009).

[25] T. Kodaira, Y. Nozue, S. Ohwashi, T. Goto, and O. Terasaki, Phys. Rev. B **48**, 12 245 (1993).

[26] F. Izumi and T. Ikeda, Mater. Sci. Forum **321–324**, 198 (2000).